THE JOURNAL OF BIOLOGICAL CHEMISTRY VOL. 287, NO. 19, pp. 15635–15647, May 4, 2012

TDP-43 and FUS RNA-binding Proteins Bind Distinct Sets of Cytoplasmic Messenger RNAs and Differently Regulate Their Post-transcriptional Fate in Motoneuron-like Cells*[S]

Received for publication, December 15, 2011, and in revised form, March 14, 2012 Published, JBC Papers in Press, March 16, 2012, DOI 10.1074/jbc.M111.333450

Claudia Colombrita[‡1], Elisa Onesto[‡1], Francesca Megiorni[§], Antonio Pizzuti[§], Francisco E. Baralle[¶], Emanuele Buratti[¶], Vincenzo Silani[‡‖], and Antonia Ratti[‡‖2]

From the [‡]Department of Neurology and Laboratory of Neuroscience, IRCCS Istituto Auxologico Italiano, Milan 20149, Italy, [§]Department of Experimental Medicine, Sapienza University of Rome, Rome 00161, Italy, [¶]International Centre for Genetic Engineering and Biotechnology, AREA Science Park, Trieste 34149, Italy, and the [‖]Department of Neurological Sciences, "Dino Ferrari" Center, Università degli Studi di Milano, Milan 20122, Italy

Background: The RNA-binding proteins TDP-43 and FUS form abnormal aggregates in patients with amyotrophic lateral sclerosis and frontotemporal lobar dementia.
Results: We identified the mRNAs associated to these proteins in the cytoplasm of NSC-34 cells.
Conclusion: TDP-43 and FUS recognize distinct transcripts and differently regulate their fate.
Significance: Our results clarify TDP-43 and FUS role in neuronal metabolism and neurodegeneration.

The RNA-binding proteins TDP-43 and FUS form abnormal cytoplasmic aggregates in affected tissues of patients with amyotrophic lateral sclerosis and frontotemporal lobar dementia. TDP-43 and FUS localize mainly in the nucleus where they regulate pre-mRNA splicing, but they are also involved in mRNA transport, stability, and translation. To better investigate their cytoplasmic activities, we applied an RNA immunoprecipitation and chip analysis to define the mRNAs associated to TDP-43 and FUS in the cytoplasmic ribonucleoprotein complexes from motoneuronal NSC-34 cells. We found that they bind different sets of mRNAs although converging on common cellular pathways. Bioinformatics analyses identified the $(UG)_n$ consensus motif in 80% of 3′-UTR sequences of TDP-43 targets, whereas for FUS the binding motif was less evident. By *in vitro* assays we validated binding to selected target 3′-UTRs, including *Vegfa* and *Grn* for TDP-43, and *Vps54*, *Nvl*, and *Taf15* for FUS. We showed that TDP-43 has a destabilizing activity on *Vegfa* and *Grn* mRNAs and may ultimately affect progranulin protein content, whereas FUS does not affect mRNA stability/translation of its targets. We also demonstrated that three different point mutations in TDP-43 did not change the binding affinity for *Vegfa* and *Grn* mRNAs or their protein level. Our data indicate that TDP-43 and FUS recognize distinct sets of mRNAs and differently regulate their fate in the cytoplasm of motoneuron-like cells, therefore suggesting complementary roles in neuronal RNA metabolism and neurodegeneration.

The DNA/RNA-binding protein TDP-43 represents the major component of the intracellular inclusions occurring in the brain of patients affected by a series of neurodegenerative diseases, including the majority of both familial and sporadic amyotrophic lateral sclerosis (ALS)[3] cases and a subset of Tau-negative and ubiquitin-positive frontotemporal lobar dementia (FTLD) cases (1, 2). The genetic findings of causative mutations in *TARDBP*, the gene encoding for TDP-43, in 5% of familial ALS cases further support the pathogenic role of this protein (3). Abnormal cytoplasmic aggregates of FUS, another DNA/RNA-binding protein, are observed in a subset of FTLD cases, which are Tau- and TDP-43-negative, and in 4–5% of familial ALS cases with mutations in the *FUS/TLS* gene, suggesting that dysregulation of RNA metabolism plays an important role in ALS and FTLD pathogenesis (4, 5).

TDP-43 and FUS are ubiquitously expressed and multifunctional RNA-binding proteins (RBP) with a main localization in the nucleus, where they are implicated in several steps of RNA metabolism, such as transcription, pre-mRNA splicing, and microRNA processing (6, 7). However, they also take part in other cellular processes in the cytoplasmic compartment, including mRNA transport, mRNA stability, and translation (8, 9). In fact, shuttling of these two proteins into the cytoplasm has been described, particularly in neurons, where an activity-dependent translocation of TDP-43 and FUS into dendrites was observed (10–13). This suggests that these two RBPs participate also in regulating mRNA transport into neurites and, likely, local protein synthesis at synapses, two processes that are essential to neurons for a fast response to stimuli and cell survival (14). Localization of TDP-43 and mutant FUS in stress

* This work was supported by the Italian Agency of Research on ALS (AriSLA) (Grant RBPALS) and Fondazione CARIPLO (Grant 2008-2307).
[S] This article contains supplemental Tables 1–7 and Figs. 1–5.
Microarray data are available at GEO data base (ncbi.nlm.nih.gov) under accession number GSE33159.
[1] Both authors contributed equally to this work.
[2] To whom correspondence should be addressed: Dept. of Neurology, IRCCS Istituto Auxologico Italiano, Via Zucchi, 18–20095 Cusano Milanino, Milan, Italy. Tel.: 39-02-619113045; Fax: 39-02-619113033; E-mail: antonia.ratti@unimi.it.

[3] The abbreviations used are: ALS, amyotrophic lateral sclerosis; FTLD, frontotemporal lobar dementia; RBP, RNA-binding protein; RNP, ribonucleoprotein; IP, immunoprecipitation; RIP-chip, RNA immunoprecipitation and chip analysis; CLIP, cross-linking and immunoprecipitation; PAR-CLIP, photoactivatable ribonucleoside-enhanced CLIP; MEME, multiple expectation maximization for motif elicitation; RSAT, regulatory sequence analysis tools; PGRN, progranulin; OPTN, optineurin.

granules, ribonucleoprotein (RNP) complexes that negatively control mRNA translation in condition of cellular insults, has been recently and widely demonstrated (15–17), supporting an additional role of TDP-43 and FUS in the cytoplasmic compartment in association with translation.

To date, however, disease mechanisms for these two RBPs have not been clearly elucidated. Mislocalization and aggregation of TDP-43 and FUS in the cytoplasm of ALS/FTLD-affected neurons are supposed to trigger neurodegeneration by loss of their biological functions ("loss-of-function" hypothesis) and/or by acquisition of potentially toxic functions in the cytoplasm ("gain-of-function" hypothesis) (18). An important issue in understanding the pathogenic mechanisms in ALS and FTLD is certainly the full definition of the transcripts that are directly bound and post-transcriptionally regulated by TDP-43 and FUS in association with splicing and, in particular in neuronal cells, with mRNA transport, stabilization, and/or translational processes.

Interestingly, using high throughput RNA/DNA sequencing technologies coupled to immunoprecipitation (RIP-seq) or cross-linking and immunoprecipitation (PAR-CLIP/iCLIP/CLIP-seq), recent papers have identified large sets of putative TDP-43 and FUS RNA targets in neuronal and non-neuronal cells (19–23). These studies revealed that TDP-43 and FUS are mainly involved in pre-mRNA splicing, as target sequences were preferentially localized in long intronic regions and near splice site acceptors, respectively. From these findings, however, it emerged that about 5–16% of all TDP-43 and FUS target sequences also mapped in exonic regions, with a high enrichment in 3′- untranslated region (UTR) sequences (3–12%) (19–23). In general, regulatory *cis*-acting elements, usually present in the 3′-UTR but sometimes also located in the 5′-UTR or in the coding sequence of target mRNAs, are responsible for RBP-mediated transport of mRNAs and post-transcriptional regulation of gene expression together with miRNA *trans*-acting factors (24). The importance of TDP-43 and FUS binding to 3′-UTR regulatory sequences has been highlighted by the observation that TDP-43 can auto-regulate its own protein levels by binding to its 3′-UTR sequence in a negative feedback loop (25), whereas FUS was shown to transport the actin-related *Nd1-L* mRNA into dendrites by binding to its 3′-UTR (12).

As TDP-43 and FUS share many common functional and biochemical features, we performed a RIP-chip analysis to identify and compare the biological mRNA targets of these two RBPs associated with RNP complexes in the cytoplasm of motoneuronal NSC-34 cells with the final aim of unraveling their potential role in mRNA transport, stability, and translation in neurons.

EXPERIMENTAL PROCEDURES

Cell Culture—The mouse motoneuronal cell line NSC-34 (a kind gift of N. R. Cashman, University of British Columbia, Vancouver, Canada) was cultured in DMEM supplemented with 5% fetal bovine serum, 1 mM sodium pyruvate, 100 units/ml penicillin, and 100 μg/ml streptomycin as previously reported (26). All reagents were purchased from Sigma.

RNP Isolation and RNA Immunoprecipitation (RIP)—Isolation of endogenous RNP complexes for RIP-chip analysis was conducted as already described (26). Briefly, 8×10^6 NSC-34 cells were harvested and resuspended in RNP buffer (100 mM KCl, 5 mM $MgCl_2$, 10 mM HEPES, pH 7.4, 0.5% Nonidet P-40, 10 μM DTT) plus 400 units of RNase inhibitor (Promega) and a protease inhibitory mixture (Roche Applied Science). NSC-34 lysate (1.2 mg) was incubated for 2 h at room temperature in NT2 buffer (50 mM Tris-HCl, pH 7.4, 150 mM NaCl, 1 mM $MgCl_2$, 1 mM DTT, 20 mM EDTA, 0.05% Nonidet P-40) together with protein G-Sepharose beads (GE Healthcare) precoated overnight with 8 μg of anti-TDP-43 (ProteinTech Group), anti-FUS (Abcam), or anti-IgG (Santa Cruz Biotechnology) antibodies. After washes with ice-cold NT2 buffer, mRNA was phenol-chloroform-extracted from immunoprecipitated RNPs after digestion with proteinase K for 30 min. In parallel, proteins recovered from immunoprecipitated RNPs were analyzed by Western blotting.

Western Blotting—NSC-34 cells were homogenized in lysis buffer (150 mM NaCl, 20 mM Tris-HCl, pH 7.4, 1% Triton X-100, protease inhibitor mixture) and incubated for 15 min on ice. Protein lysates (30 μg) were resolved on 10% SDS-PAGE and transferred to nitrocellulose membrane. The nuclear fraction was obtained by the ProteoJET Cytoplasmic and Nuclear Protein Extraction kit (Fermentas Life Sciences). Immunoblots were performed with anti-TDP-43, VPS54, and ATXN2 (ProteinTech Group), FUS (BD Transduction Laboratories), VEGF (Millipore), Progranulin (PGRN; R&D Systems), Optineurin (OPTN; Abcam), and Histone H1 and α-Tubulin (Santa Cruz Biotechnology) antibodies. The ECL Plus kit (GE Healthcare) was used for chemiluminescence detection. Densitometric analyses were performed using QuantityOne software (Bio-Rad).

Chip Analysis—Phenol-chloroform-extracted mRNA (~100 ng) from RIP experiments in triplicate was amplified and biotinylated using the TotalPrep RNA Amplification kit (Ambion) according to the manufacturer's directions. Briefly, first- and second-strand reverse transcription steps were performed followed by a single *in vitro* transcription amplification step to generate biotin-16-UTP-labeled cRNA. RNA integrity was evaluated before and after labeling using the Agilent 2100 Bioanalyzer (Agilent Technologies). 750 ng of cRNA per sample were hybridized to the Illumina MouseRef-8 v2.0 BeadChips (Illumina), containing about 25,600 well-annotated RefSeq transcripts. BeadChips were scanned using the BeadArray Reader (Illumina). The GenomeStudio software (Illumina) was used to extract raw data for statistical analysis. Data were normalized using the quantile normalization method, and a multiple testing correction using Benjamini and Hochberg False Discovery Rate was applied. Genes in the TDP-43- or FUS-IP samples presenting with a q-value <0.05 were considered significantly different compared with control samples immunoprecipitated with an irrelevant antibody. A *bona fide* enrichment of specific transcripts in TDP-43-/FUS-IP *versus* control-IP was obtained when stringent conditions were applied (-fold change >3). Microarray data are available at GEO data base (ncbi.nlm.nih.gov) under the accession number GSE33159.

Bioinformatic Analysis—Functional annotation study of RIP-chip data were conducted using the on-line DAVID analysis tool (david.abcc.ncifcrf.gov), and only Gene Ontology categories with a p value <0.05 were considered significantly represented.

We used MEME (Multiple EM for Motif Elicitation)-Chip Version 4.6.1 (27), a section of the MEME local search method (28), for discovering motifs in the large sets of RIP-chip identified sequences, as there is no upper limit on the number or size of the submitted FASTA nucleotides. We focused on the 3′-UTR of TDP-43 or FUS mRNA targets retrieving Refseqs from the UTRdb data base (67). MEME was instructed to report the top 6 motifs between 6 and 20 bases in length. We accepted motifs that showed an e value $<1.0e-006$. Prediction of over-represented *cis*-regulatory elements shared by TDP-43 or FUS bound mRNAs was also obtained by RSAT (Regulatory Sequence Analysis Tools), a word-enumeration algorithm, which was also used to match for specific functional motifs (accepted score ≥ 0.89 with 1–2 allowed mismatches). The research of the GGUG element in the 3′-UTRs of FUS targets was performed by RSAT "pattern matching" with 0 mismatches.

Plasmid Constructs—The 3′-UTR sequences of the RIP-identified targets were RT-PCR-amplified from mouse NSC-34 total RNA (primer sequences are available in supplemental Table 6) and subsequently cloned into pCRII vector (Invitrogen) or pJet1.2/blunt vector (Fermentas Life Science) for *in vitro* transcription. For luciferase reporter assays, the full-length *Vegfa* and *Grn* 3′-UTR sequences were cloned into the pmirGLO dual-luciferase vector (Promega) at the 3′ end of the firefly gene. All clones and their orientation were validated by DNA sequencing. The FLAG-tagged wild-type and deleted (ΔRRM1) human TDP-43 (hTDP-43) plasmids were previously described (29). The FLAG-tagged mutant (p.Q331K, p.M337V, p.A382T) TDP-43 constructs were a kind gift of W. Rossoll (Emory University School of Medicine, Atlanta, GA).

In Vitro Transcription, UV Cross-linking and IP (UV-CLIP)—Radiolabeled riboprobes were obtained by *in vitro* transcription of 0.5 μg of restriction enzyme-linearized 3′-UTR DNA construct using 20 μCi of [α-^{32}P]UTP per reaction. The resulting riboprobes were purified on ProbeQuant G-50 microcolumns (GE Healthcare). UV-CLIP experiments with transfected and non-transfected NSC-34 protein lysates were performed as previously described (26) using anti-TDP-43, anti-FUS (Abcam), anti-FLAG (Sigma), or the irrelevant anti-IgG antibodies for immunoprecipitation (IP).

For competition assays, 1×10^6 cpm ^{32}P-labeled riboprobe were incubated with 500 ng of the recombinant GST-TDP-43 protein, obtained as previously described (30), and increasing amounts (2.5, 10, and 100 ng) of unlabeled $(UG)_6$ or scrambled N_{12} ribonucleotides for 10 min at room temperature in 25 μl of binding buffer (1.3 mM $MgCl_2$, 19 mM HEPES-KOH, pH 7.4, 1.5 mM ATP, 19 mM creatine phosphate). After irradiation with UV (Stratalinker, Stratagene) for 5 min on ice and RNase A treatment (25 units) for 30 min, samples were then resolved on 10% SDS-PAGE and visualized by autoradiography.

Gene Silencing and Cell Treatments—For gene silencing experiments the following siRNA duplexes were used: 5′-CGAUGAACCCAUUGAAAUAdTdT-3′ for mouse TDP-43 (Mission siRNA, Sigma), a mix of 5′-GAAUUCUCUGGGAAUCCUAdTdT-3′ and 5′-GUGGUUAUGGCAAUCAGGAdTdT-3′ for mouse FUS (Mission siRNA; Sigma), and Stealth siRNA low GC (Invitrogen) as a negative control. NSC-34 cells were transfected with 40 nM concentrations of the indicated siRNA duplexes in a double round of transfection using Lipofectamine 2000 (Invitrogen) according to the manufacturer's instructions. After a 48- or 96-h gene silencing for FUS and TDP-43, respectively, both target gene and control siRNA-treated cells were harvested or exposed to 50 μM 5,6-dichlorobenzamidazole riboside (Sigma) for the indicated times.

TDP-43 Overexpression and Rescue Experiments—NSC-34 cells were mock- or FLAG-hTDP-43- transfected for 48 h using Lipofectamine 2000. For rescue experiments, after 48-h of TDP-43 gene silencing, NSC-34 cells were retransfected with FLAG-hTDP-43 construct and recovered after 24 h for protein analysis.

Real Time Quantitative PCR—Total RNA from NSC-34 cells was extracted by TRIzol reagent (Invitrogen) according to the manufacturer's recommendations. Retro-transcription of mRNA was performed after DNase I (Roche Applied Science) treatment using SuperScriptII RT (Invitrogen) and oligo(dT) primers. Oligonucleotide pairs for each gene were designed with Primer Express 3.0 software (Applied Biosystems) on exon boundaries (for primer sequences, see supplemental Table 7). Real time PCR was performed for 45 cycles with SYBR Green PCR Master mix (Applied Biosystems) and processed on ABI Prism 7900HT (Applied Biosystems). Reactions were run in triplicate for each sample, and a dissociation curve was generated at the end. Threshold cycles (C_t) for each tested gene were normalized on the housekeeping *Rpl10a* gene value (ΔC_t), and every experimental sample was referred to its control ($\Delta\Delta C_t$). For mRNA decay assay, ΔC_t at each indicated time was referred to ΔC_t at time 0. Fold change values were expressed as $2^{-\Delta\Delta Ct}$.

Luciferase Assay—For luciferase experiments NSC-34 cells were plated in duplicate for each experimental condition, and after 48 h of TDP-43- or control-siRNA transfection, cells were retransfected with 500 ng of each firefly luciferase-3′-UTR construct (pmirGLO-*Vegfa* and pmirGLO-*Grn*) using Lipofectamine 2000. Measurement of the luciferase activity was performed using the Dual Luciferase Reporter Assay System (Promega) 72 h after the initial siRNA transfection. The firefly luciferase activity of *Vegfa* and *Grn* 3′-UTR constructs was normalized against the Renilla luciferase output of the same pmirGLO constructs.

Statistical Analysis—Statistical analysis was conducted with PRISM software (GraphPad) using two-tailed Student's t test or one-way analysis of variance.

RESULTS

Identification of TDP-43 and FUS mRNA Targets by RIP-chip Analysis—RIP-chip analysis of cytoplasmic RNP complexes from motoneuron-like NSC-34 cells was carried out to define the mRNA targets of TDP-43 and FUS in the cytoplasmic compartment, which are likely to be transported into neurites and/or locally translated at synapses. We first confirmed that

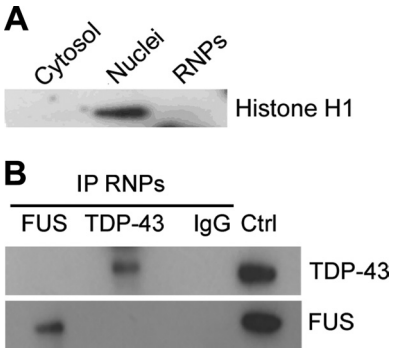

FIGURE 1. **Isolation of the cytoplasmic RNP complexes containing TDP-43 and FUS.** *A*, shown is immunoblot analysis with Histone H1 antibody as a nuclear marker. *B*, shown is a representative Western blot of RNP complexes immunopurified from cytoplasmic fraction with anti-TDP-43 (*upper inset*) and anti-FUS (*lower inset*) antibodies in NSC-34 cells. The irrelevant IgG antibody was used as negative control for IP assays. Total cell lysate was loaded as a positive control (*Ctrl*).

our extraction method allowed the isolation of the cytoplasmic RNP complexes with no contamination of nuclear components using the Histone H1 as a nuclear marker in immunoblot analysis (Fig. 1*A*). We also tested the specificity of the IP assays for TDP-43 and FUS proteins by immunoblotting an aliquot of each experiment before proceeding with the chip analysis. We proved that the endogenous RNP complexes were efficiently isolated and that TDP-43 and FUS proteins did not usually associate in the same RNP particle, being their co-localization rarely observed (Fig. 1*B*; data not shown). To identify the transcripts contained and bound in such RNP complexes, a chip analysis was performed using the recovered mRNAs from RIP experiments in triplicate.

Statistical analysis of the data showed that all the TDP-43-IP samples, the FUS-IP samples, and the control-IP samples clearly fell into distinct hierarchical clusters (data not shown). With regard to TDP-43, a set of 204 genes significantly enriched in TDP-43-IP *versus* control-IP ($q < 0.05$) was identified. Interestingly, 194 of 204 were enriched by more than 2-fold (fold change >2) in TDP-43 IP *versus* control IP, confirming the enrichment in TDP-43 targets using our RIP procedure. When we applied more stringent conditions and arbitrarily assigned a fold change >3, a pool of 168 distinct genes were defined as *bona fide* TDP-43 mRNA targets (supplemental Table 1) and used for subsequent bioinformatics analyses. We found overlapping with some genes recently identified by RIP-seq and CLIP-seq approaches by other groups (supplemental Table 1) (19–21).

In parallel, statistical analysis of FUS-IP samples identified a set of 777 transcripts significantly enriched *versus* control-IP (fold change >3; $q < 0.05$) (supplemental Table 2). Comparison of our RIP-chip data with FUS RNA targets recently defined by PAR-CLIP assay revealed that 486/777 (63%) were in common in motoneuronal NSC-34 and non-neuronal HEK293 cells (supplemental Table 2) (23).

Functional Annotation Analysis of RIP-chip Identified Targets—Although TDP-43 and FUS RBPs share many biochemical features and functional similarities, no common mRNA targets were identified in our analyses. However, *in silico* functional annotation analysis by DAVID program

TABLE 1
Functional annotation analysis of TDP-43 and FUS mRNA targets

1A. Functional categories for TDP-43 mRNA targets			
GO Categories	**GO Term**	**Gene Count**	**p-value**
Biological process			
wnt receptor signaling pathway	GO:0016055	5	2.06E-02
regulation of transcription*	GO:0045449	27	2.78E-02
neuron differentiation	GO:0030182	8	4.15E-02
- dendrite development	GO:0016358	4	3.72E-03
Molecular Function			
GTPase regulator activity*	GO:0030695	10	3.43E-03
purine ribonucleotide binding*	GO:0032555	24	2.51E-02

1B. Functional categories for FUS mRNA targets			
GO Categories	**GO Term**	**Gene Count**	**p-value**
Biological process			
regulation of transcription*	GO:0045449	142	2.53E-12
- negative regulation of transcription from RNA polymerase II promoter	GO:0000122	15	4.17E-02
cell cycle	GO:0007049	54	2.80E-09
- mitosis	GO:0007067	15	9.31E-03
ribonucleoprotein complex biogenesis	GO:0022613	22	2.08E-08
- ribosome biogenesis	GO:0042254	16	1.21E-05
- rRNA processing	GO:0006364	8	1.74E-02
- spliceosome assembly	GO:0000245	4	1.55E-02
RNA processing	GO:0006396	41	6.63E-08
- RNA splicing	GO:0008380	25	2.79E-07
cellular response to stress	GO:0033554	35	4.39E-06
- DNA repair	GO:0006281	22	5.73E-05
proteolysis involved in cellular protein catabolic process	GO:0051603	41	1.08E-05
- ubiquitin-dependent protein catabolic process	GO:0006511	17	5.09E-05
chromosome organization	GO:0051276	34	1.14E-05
- chromatin modification	GO:0016568	24	1.59E-05
methylation	GO:0032259	9	7.66E-03
Molecular Function			
purine ribonucleotide binding*	GO:0032555	107	4.30E-07
- ATP binding	GO:0005524	93	9.90E-08
translation initiation factor activity	GO:0003743	10	4.30E-04
double-stranded RNA binding	GO:0003725	7	1.39E-03
helicase activity	GO:0004386	14	9.84E-04
- ATP-dependent helicase activity	GO:0008026	11	1.26E-03
protein serine/threonine kinase activity	GO:0004674	30	9.95E-04
GTPase regulator activity*	GO:0030695	26	2.03E-03
- Ras GTPase activator activity	GO:0005099	7	3.28E-02
- Rab GTPase activator activity	GO:0005097	6	2.06E-02

* Common Gene Ontology categories for TDP-43 and FUS.

revealed that some TDP-43 and FUS targets belonged to common Gene Ontology categories, including regulation of transcription, GTPase regulator activity, and purine ribonucleotide binding (Table 1). TDP-43 mRNA targets were particularly enriched for Gene Ontology terms related to neuron differentiation and dendrite development as well as Wnt receptor signaling pathway (Table 1A), whereas FUS targets to cell cycle, ribonucleoprotein complex biogenesis (ribosome biogenesis and spliceosome assembly), RNA processing and splicing, cellular response to stress and DNA repair, ubiquitin-dependent proteolysis, chromosome organization and methylation (Table 1B). Also the KEGG (Kyoto Encyclopedia of Genes and Genomes) data base revealed that FUS mRNA targets were significantly represented in two pathways, the spliceosome (supplemental Fig. 1) and the ubiquitin-mediated proteolysis. In particular, the FUS mRNA targets involved in the latter pathway included five different Cullins (1–5) that contribute to form the multisubunit RING-finger type ubiquitin-ligase E3 (supplemental Fig. 2).

Search for Consensus Binding Motifs in 3′-UTR Sequences of RIP-chip-identified Targets—Because the 3′-UTR sequences usually contain *cis*-acting regulatory elements responsible of

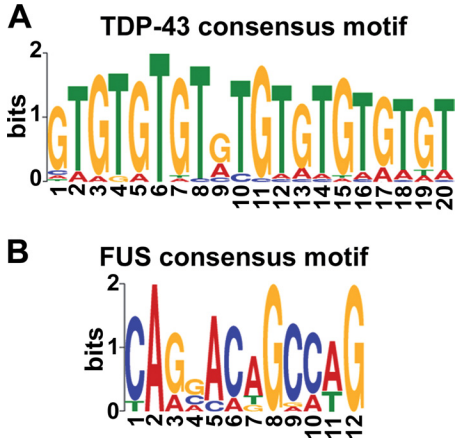

FIGURE 2. **Identification of consensus sequence motifs in the 3′-UTR of TDP-43 and FUS mRNA targets.** *A*, shown is the consensus sequence logo as predicted by MEME analysis of the 3′-UTR sequences of TDP-43 targets. The $(TG)_n$ motif (*e* value <1.0*e*−100; *p* value<1.0*e*−07) is present in 80% of RIP-identified targets. *B*, shown is the consensus sequence logo predicted for FUS targets (*e* value <1.0*e*−007; *p* value <1.0*e*−05) and identified in only 9.6% of 3′-UTR sequences. In each *column*, all letters with observed frequencies greater than 0.2 are shown. *Single letters* match that letter.

RBP binding, we analyzed TDP-43 and FUS mRNA targets identified by RIP-chip for the presence of significantly enriched sequence motifs in such regions. The 3′-UTR lengths ranged from 59 bp (*Cfp*) to 6,350 bp (*Unc5c*) for TDP-43 targets and from 58 bp (*Dnajc2*) to 14,162 bp (*Strbp*) for FUS targets.

We performed *in silico* motif-based sequence analysis using the MEME-ChIP program, which applies the expectation maximization algorithm to find the maximum likelihood motif estimation and directly processes large input datasets. The software identified the $(TG)_n$ motif (*e* value <1.0*e*−100; *p* value <1.0*e*−07), the already known and well established sequence signature for TDP-43 (30, 31), among the 3′-UTRs of TDP-43 targets identified by RIP-chip (Fig. 2*A*). RSAT pattern matching analysis allowed determination of the occurrence of this *cis*-acting element in 79.8% (134/168) of the submitted TDP-43 mRNA targets (supplemental Table 3). In particular, $(TG)_n$ repeats ($n = 6–10$) were present in 124 different sequences and the related motif $(TG)_nTA(TG)_m$ ($n = 0–5$; $m = 0–5$) (19) in 10 additional 3′-UTRs. MEME analysis revealed other two significantly enriched motifs, although with lower *e* values, consisting of an A-rich element (*e* value <1.0*e*−010; *p* value <1.0*e*−05) and a T-rich element (*e* value <1.0*e*−006; *p* value <1.0*e*−05) in smaller subsets of targets (35.7 and 26.7%, respectively), often co-existing with the $(TG)_n$ motif (data not shown). The "motif discovery" tool by RSAT, which uses a non-probabilistic algorithm to search for *de novo* consensus motifs, confirmed that all the three pattern sequences discovered by MEME were significantly over-represented in the 3′-UTR of TDP-43 ligands.

Concerning the FUS mRNA targets identified by RIP-chip, the MEME-ChIP algorithm found one weakly enriched motif endowed with G/C nucleotides (*e* value <1.0*e*−007; *p* value <1.0*e*−05) that was present in 9.6% of the analyzed sequences (Fig. 2*B*), suggesting that particular conformational structures of the target mRNAs rather than specific sequence motifs are likely needed for FUS binding, as already hypothesized (12, 23). By RSAT we also tested the enrichment of the GGUG motif, previously reported to be recognized by FUS (32), but we did not find such motif to be significantly represented in the 3′-UTR of our RIP-chip-identified set of transcripts.

Validation of TDP-43 and FUS Binding to Their Target 3′-UTR Sequences—Our RIP-chip data for TDP-43 and FUS have confirmed some of the RNA targets recently identified by other groups with different experimental approaches (supplemental Tables 1 and 2) (19–21, 23). However, such RNA targets were neither unambiguously identified, nor was the binding site precisely mapped also using high throughput RNA-sequencing, highlighting the limits of each experimental approach used (supplemental Table 4). To definitively prove that our RIP-chip-identified transcripts represented specific ligands and that the 3′-UTR was really responsible of this binding, we selected some targets to be validated by means of protein/RNA binding assays.

On the basis of their already reported genetic association to ALS or FTLD diseases, *Vegfa* (vascular endothelial growth factor a) and *Grn* (progranulin) transcripts were considered among all the TDP-43 targets (33–35), whereas *Atxn2* (Ataxin 2), *Optn* (optineurin), *Taf15* (TBP-associated factor 15 RNA-polymerase II), and *Vps54* (vacuolar protein sorting 54) transcripts were chosen for FUS (36–39) (Fig. 3*A*). Additionally, we considered also *Gemin7* and *Nrp* (neural regeneration protein) for TDP-43 and *Nvl* (nuclear VCP-like) for FUS because of their potential or already documented involvement in neuronal metabolism (40–42) (Fig. 3*A*). As regards the selected TDP-43 mRNA targets, *Vegf* and *Grn* were identified also by other groups (supplemental Table 4), whereas for FUS all the selected targets but one (*Optn*) have been recently identified also by Hoell *et al.* (23) (supplemental Table 5).

Radiolabeled riboprobes corresponding to the selected target 3′-UTR sequences were used in UV-CLIP experiments using NSC-34 protein lysates. In this way, we confirmed TDP-43 binding to all the tested transcripts (Fig. 3*B*), including *Gemin7* and *Nrp*, which in contrast to *Vegfa* and *Grn* did not contain the consensus $(TG)_n$ binding repeat. On the other hand, FUS was shown to bind to *Vps54*, *Nvl*, and *Taf15* 3′-UTRs (Fig. 3*C*) but not to *Atxn2* and *Optn* (data not shown).

Mapping of TDP-43 Binding Site in Vegfa and Grn 3′-UTR Sequences—Because the RRM1 (RNA recognition motif 1) domain of TDP-43 is responsible of RNA binding (30), we investigated whether its disruption might determine a defective *Vegfa* and *Grn* mRNA binding. We transfected NSC-34 cells with FLAG-tagged wild-type or ΔRRM1 (lacking the entire RRM1 domain) TDP-43 construct (Fig. 4*A*). UV-CLIP assays were performed using such cell lysates, radiolabeled *Vegfa* and *Grn* 3′-UTR riboprobes, and anti-FLAG antibody to immunoprecipitate recombinant TDP-43 proteins. Using this approach we demonstrated that the RRM1 domain was responsible of TDP-43 binding to both *Vegfa* and *Grn* 3′-UTR sequences because its deletion abolished binding of these targets (Fig. 4*B*).

Because *Vegfa* and *Grn* mRNAs contained the consensus $(TG)_n$ binding motif in their 3′-UTR sequence, we tested whether TDP-43 binding was specific by competition experiments. We performed UV cross-linking assays using recombinant TDP-43 protein and radiolabeled *Vegfa* and *Grn* 3′-UTR riboprobes in the presence of increasing amounts of unlabeled

A

Gene	Symbol	RefSeq ID	TDP-43-IP FC	FUS-IP FC	Neurodegenerative disease	References
Vascular endothelial growth factor a	*Vegfa*	NM_001025250.3	3.2		ALS	33 43
Neural regeneration protein	*Nrp*	NM_001013372.2	5.5			41
Progranulin	*Grn*	NM_008175.4	7.9		ALS, FTLD	34 35 44
Gemin 7	*Gemin7*	NM_027189.2	10.6		SMA	40
Optineurin	*Optn*	NM_181848.4		4.4	ALS	37
Nuclear VCP-like	*Nvl*	NM_026171		4.5		42
Vacuolar protein sorting 54	*Vps54*	NM_139061		5.9	ALS	39
Ataxin 2	*Atxn2*	NM_009125		7.7	ALS, SCA2	36
TAF15 RNA polymerase II	*Taf15*	NM_027427		8.3	ALS	38

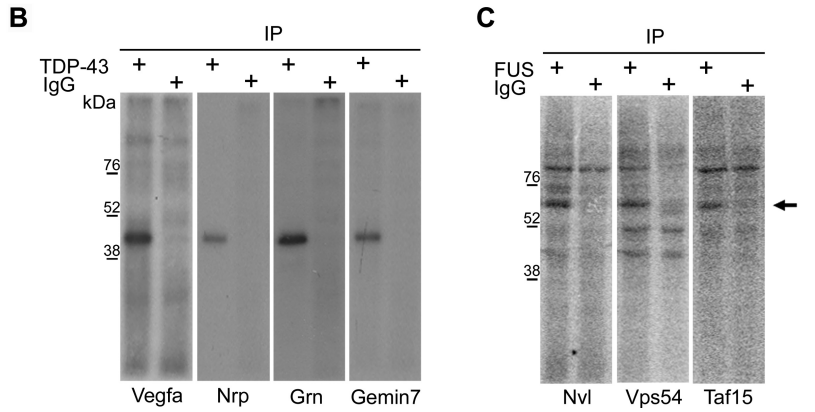

FIGURE 3. **Validation of TDP-43 and FUS binding to selected mRNA targets by UV-CLIP assays.** *A*, shown is a list of the RIP-chip-identified targets of TDP-43 and FUS selected for further validation. *FC*, fold change value corresponding to the enrichment value for TDP-43-IP or FUS-IP compared with control IgG-IP; *SCA2*, spinocerebellar ataxia 2. *B*, shown is SDS-PAGE of UV-CLIP experiment with TDP-43 antibody and radiolabeled *Vegfa* (*first lane*), *Grn* (*third lane*), *Gemin7* (*fifth lane*), or *Nrp* (*seventh lane*) 3′-UTR riboprobes; the isotypic IgG antibody was used as a negative control (*second*, *fourth*, *sixth*, and *eighth lanes*). *C*, shown is SDS-PAGE of the UV-CLIP experiment with FUS antibody and radiolabeled *Vps54* (*first lane*), *Nvl* (*third lane*), or *Taf15* (*fifth lane*) 3′-UTRs; the isotypic IgG antibody was used as a negative control (*second*, *fourth*, and *sixth lanes*). The *arrow* indicates a FUS-containing RNP complex with an apparent molecular mass of 65 kDa. The 3′-UTR riboprobes in *B* and *C* were generated according to the GenBank™ Reference Sequences indicated in *A*.

$(UG)_6$ or scrambled (N_{12}) oligoribonucleotides. We found that only the $(UG)_6$ oligoribonucleotide was able to compete with the target sequences for binding to TDP-43 protein (Fig. 4*C*).

As *Vegfa* and *Grn* are genetically associated to ALS and FTLD as susceptibility and causative genes, respectively (33–35, 43, 44), we mapped TDP-43 binding site more precisely to investigate whether and how TDP-43 binding to *Vegfa* and *Grn* 3′-UTRs might also contribute, by post-transcriptional regulatory mechanisms, to influence their gene expression.

According to the presence of putative $(TG)_n$ consensus binding sequences, we generated distinct radiolabeled deletion fragments of *Vegfa* and *Grn* 3′-UTRs (Figs. 4, *D* and *F*), which were then used in UV-CLIP assays with NSC-34 protein lysates. Using this approach, we demonstrated that TDP-43 binding to *Vegfa* 3′-UTR mapped within a 154-nucleotide-long sequence endowed with a canonical $(TG)_{22}$ repeat (Fig. 4*E*). Similarly, TDP-43 binding to *Grn* 3′-UTR mapped to a 72-nucleotide-long sequence containing a canonical $(TG)_6$ repeat within a larger consecutive 26-nucleotide-long region enriched in G/T nucleotides (Fig. 4*G*). Interestingly, *Vegfa* and *Grn* 3′-UTR sequences are highly conserved between mouse and man (84 and 80%, respectively), including the *Grn* 26-nucleotide-long region containing the $(TG)_6$ motif (supplemental Fig. 3). On the contrary, the murine *Vegfa* $(TG)_{22}$ repeat is not conserved in humans, although a canonical $(TG)_6$ motif within a 24-nucleotide-long sequence with an interrupted $(TG)_n$ repeat was present 230 nucleotides upstream if compared with the murine orthologous gene (supplemental Fig. 4).

Finally, we also checked whether TDP-43 binding to *Grn* 3′-UTR might potentially interfere with the binding of other recognized *trans*-acting factors, such as miR-29b and miR-659, two highly conserved microRNAs already reported to inhibit post-transcriptionally *Grn* expression (45, 46). The recognition binding sites of miR-29b and miR-659 did not seem to overlap with TDP-43 binding site (supplemental Fig. 3).

Effect of TDP-43 and FUS on Stability of Their Target mRNAs—Our and previous findings of TDP-43 and FUS binding not only to introns but also to regulatory 3′-UTR sequences (12, 25, 47) and

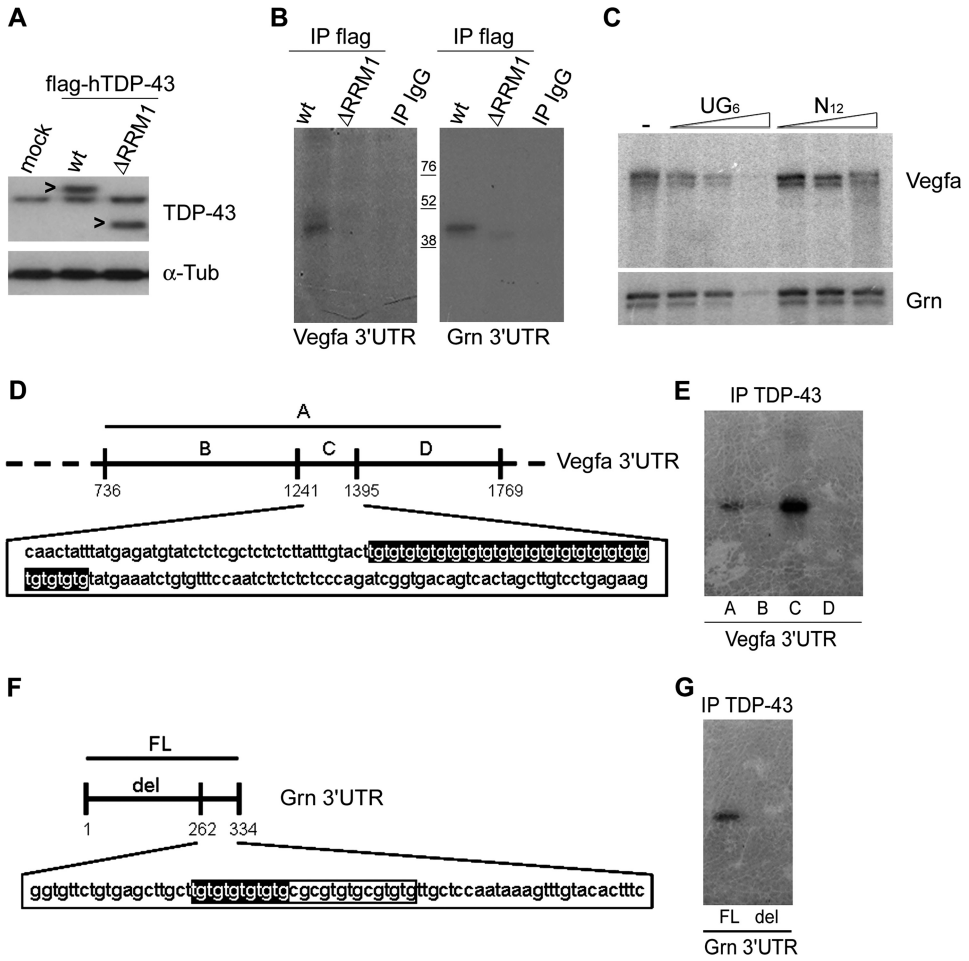

FIGURE 4. **TDP-43 specifically binds $(UG)_n$ motifs in *Vegfa* and *Grn* 3′-UTR sequences.** *A*, shown is a representative Western blot of TDP-43 in cell lysates of mock, wt, or ΔRRM1 FLAG-hTDP-43-transfected NSC-34 cells (the *arrowhead* indicates FLAG-hTDP-43 protein). *Tub*, tubulin. *B*, shown is SDS-PAGE of UV-CLIP experiment with wt or ΔRRM1 FLAG-hTDP-43 and the radiolabeled *Vegfa* (*left panel*) and *Grn* (*right panel*) 3′-UTR riboprobes. The isotypic IgG antibody was used as a negative control. *C*, shown are SDS-PAGE of UV cross-linking assays using GST-hTDP-43 protein and radiolabeled *Vegfa* and *Grn* 3′-UTR riboprobes (*first lanes*) in the presence of increasing amounts (2.5, 10, and 100 ng) of unlabeled $(UG)_6$ (*second*, *third*, and *fourth lanes*) or scrambled (N_{12}) (*fifth*, *sixth*, and *seventh lanes*) oligoribonucleotides. *D*, shown is a schematic representation of the 3′ terminal portion of *Vegfa* 3′-UTR containing the $(TG)_n$ repeat. Different deletion fragments were generated (*A–D*) where only fragment *C* contained the TDP-43 consensus motif $(TG)_{22}$. *E*, shown is SDS-PAGE of UV-CLIP with TDP-43 antibody and the four different radiolabeled *Vegfa* 3′-UTR fragments described in *D*. *F*, shown is a schematic representation of *Grn* 3′-UTR. A deletion fragment (*del*) without the TDP-43 consensus motif $(TG)_6$ was generated. *G*, shown is SDS-PAGE of UV-CLIP with TDP-43 antibody and radiolabeled full length (*FL*) or deletion (del) *Grn* 3′-UTR fragments.

their localization in stress granules (15–17) strongly suggest that TDP-43 and FUS may participate also in controlling mRNA stability and/or translation.

To evaluate whether TDP-43 and FUS binding to their target 3′-UTR sequences had any influence on mRNA stability, degradation kinetics were determined after inhibition of transcription by dichlorobenzamidazole riboside agent in condition of TDP-43 or FUS knockdown. TDP-43 gene silencing in NSC-34 cells reduced both its protein and mRNA levels to 16% when compared with control samples (Fig. 5, *A–C*). Similarly, knockdown of FUS resulted in 15 and 21% of protein and mRNA content, respectively, compared with control samples (Fig. 5, *A–C*).

Decay curves showed a slower degradation kinetics for both *Vegfa* and *Grn* mRNAs upon TDP-43 depletion (Fig. 5*D*), suggesting that in normal conditions TDP-43 has a destabilizing effect on these transcripts. Conversely, the decay curves for *Vps54*, *Nvl*, and *Taf15* did not significantly change in conditions of FUS knockdown (Fig. 5*E*), suggesting that FUS does not control mRNA stability, as already reported for another previously identified target, *Nd1-L* transcript (12). We also studied the degradation kinetics of *Atxn2* and *Optn*, although, as previously showed, we had no evidence of FUS binding to their 3′-UTR sequence. No significant changes of the decay curves of these two mRNAs were found upon FUS gene silencing (data not shown).

Effect of TDP-43 on VEGF and Progranulin Protein Content—Because we found that TDP-43 controlled the mRNA stability of its targets, we evaluated whether loss of TDP-43 activity, potentially associated to TDP-43 sequestration into cytoplasmic aggregates in ALS and FTLD tissues, may ultimately affect VEGF and PGRN protein contents, which have been reported to be altered in ALS brains and cerebrospinal fluid (48, 49).

When we evaluated the endogenous levels of VEGF and PGRN proteins in NSC-34 cells after TDP-43 gene silencing, PGRN amount significantly increased (36%; $n = 5$; $p < 0.05$), whereas VEGF did not significantly differ *versus* control (Fig. 6*A*). We found that the steady-state levels of *Vegfa* (1.36 ± 0.08; mean and S.E.; $n = 5$) and *Grn* (1.20 ± 0.18) mRNAs were both

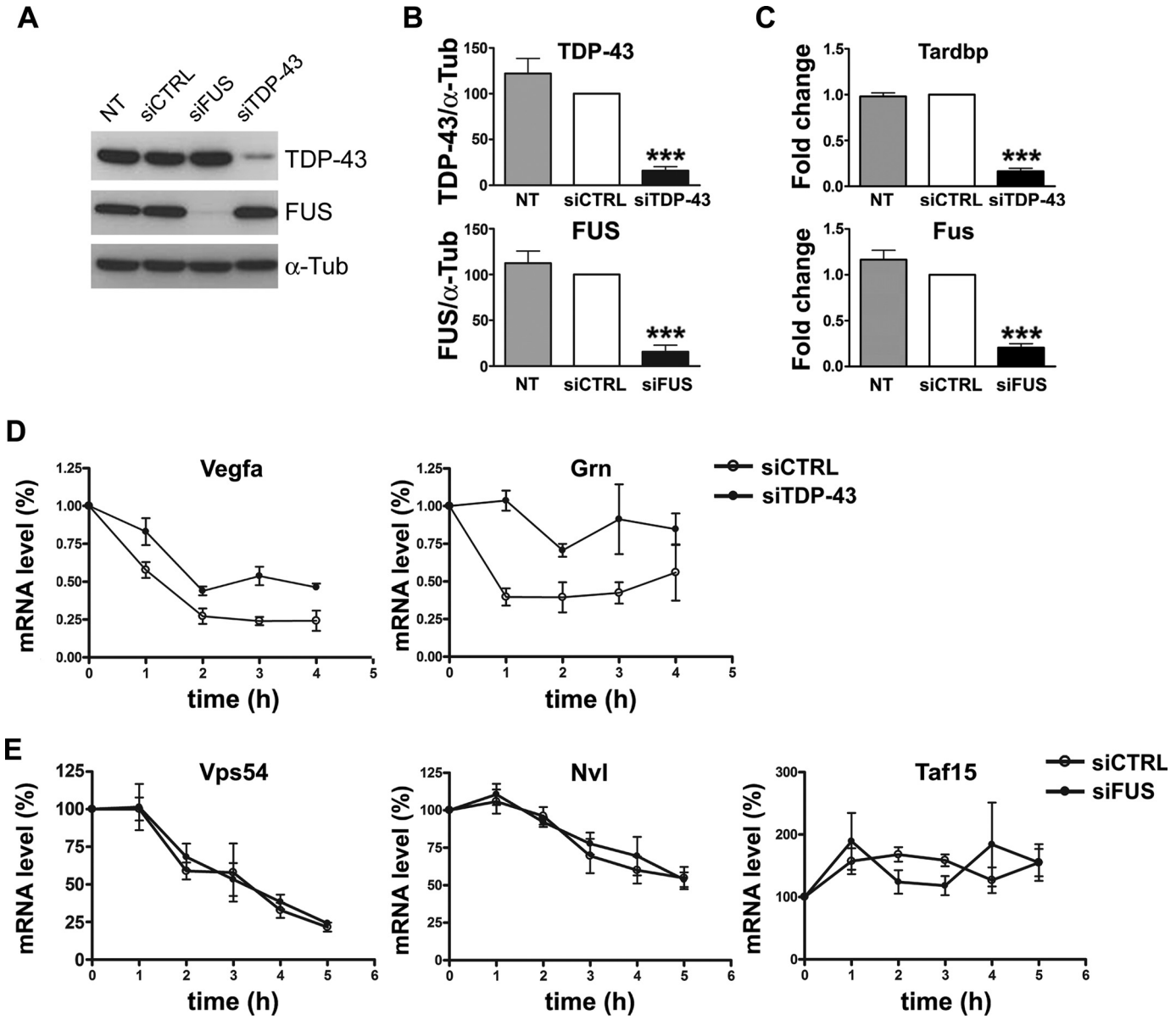

FIGURE 5. **Effect of TDP-43 and FUS on the mRNA stability of their targets.** *A*, shown is a representative Western blot of TDP-43 and FUS in cell lysates of parental (*NT*), mock-transfected (*siCTRL*), and FUS- and TDP-43-silenced (*siFUS* and *siTDP-43*, respectively) NSC-34 cells. α-Tubulin (*α-Tub*) was used for sample normalization. *B*, shown is densitometric analysis of normalized Western blot data for TDP-43 (*upper inset*) and FUS (*lower inset*) (mean ± S.E.; $n = 5$; one-way analysis of variance and Tukey post hoc test; ***, $p < 0.001$ *versus* NT and siCTRL). *C*, shown is real time PCR analysis of *Tardbp* (*upper inset*) and *Fus* (*lower inset*) mRNAs in parental (*NT*), siCTRL, and siTDP-43 or siFUS cells. Fold change values for each gene were calculated *versus* siCTRL cells (mean ± S.E.; $n = 5$; one-way analysis of variance and Tukey post hoc test; ***, $p < 0.001$ *versus* NT and siCTRL). *D* and *E*, mRNA content of the indicated gene was quantified by real time PCR in siCTRL and siTDP-43 or si-FUS NSC-34 cells after the indicated time of dichlorobenzamidazole riboside treatment. For each analyzed gene, the mRNA amount at each time point was compared with its initial mRNA level (100%) ($n = 5$; mean ± S.E.).

slightly up-regulated in conditions of TDP-43 depletion, although only *Vegfa* showed a significant increase *versus* control ($p < 0.05$) (Fig. 6*B*). To further investigate the effect of TDP-43 down-regulation on VEGF and PGRN protein synthesis, we performed luciferase assays with reporter constructs containing full-length *Vegfa* and *Grn* 3′-UTRs. We observed that luciferase values were significantly increased for both *Vegfa* (1.33 ± 0.18; $n = 7$; $p < 0.01$) and *Grn* (1.86 ± 0.26; $n = 7$; $p < 0.05$) 3′-UTR reporter constructs upon TDP-43 gene silencing in NSC-34 cells (Fig. 6*C*). This finding may be explained by the fact that the reporter construct is highly expressed in luciferase assays and may escape the finely tuned post-transcriptional regulation occurring physiologically on the long *Vegfa* mRNA.

We also evaluated the effect of TDP-43 overexpression on VEGF and PGRN protein levels. The overexpression of FLAG-tagged hTDP-43 determined a 2-fold increase in total TDP-43 content in NSC-34 cells (Fig. 7*A*). Under this condition PGRN protein levels significantly diminished to 76% in comparison to mock-transfected cells ($n = 4$; $p < 0.05$), whereas VEGF amount did not significantly vary (Fig. 7*A*). The steady-state levels of *Vegfa* and *Grn* mRNAs had comparable values in hTDP-43-over-expressing cells and in controls (Fig. 7*B*).

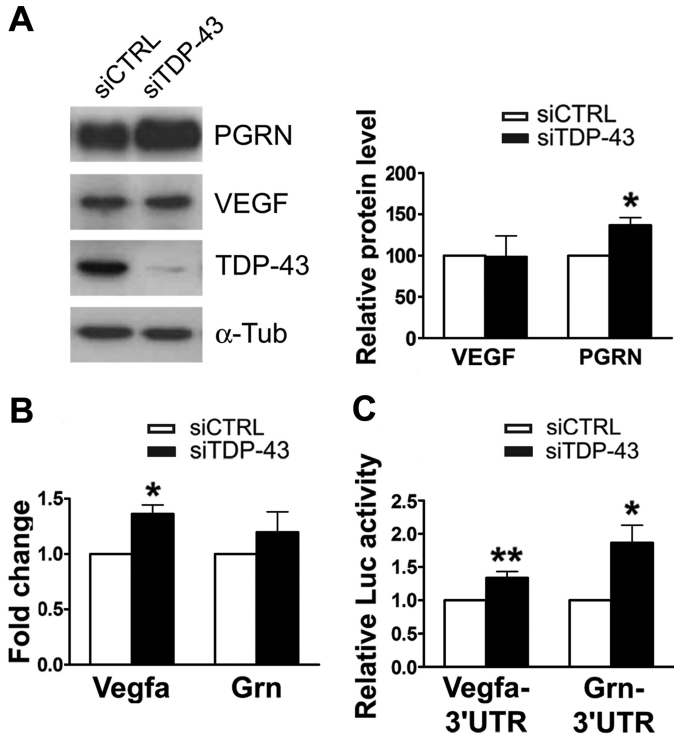

FIGURE 6. **Effect of TDP-43 on the translatability of *Vegfa* and *Grn* mRNAs.** *A*, shown is a representative Western blot of VEGF and PGRN in cell lysates of siCTRL and siTDP-43 NSC-34 cells (96-h silencing) (*left*). α-Tubulin (*α-Tub*) was used for sample normalization, and densitometric data are reported (*right*) (mean ± S.E.; $n = 5$; paired *t* test analysis; *, $p < 0.05$). *B*, real time PCR analysis of *Vegfa* and *Grn* mRNAs in siCTRL and siTDP-43 NSC-34 cells is shown. Fold change values for each gene were calculated *versus* siCTRL samples (mean ± S.E.; $n = 5$; paired *t* test analysis; *, $p < 0.05$). *C*, luciferase activity of *Vegfa*- and *Grn*-3′-UTR firefly constructs in siCTRL and siTDP-43 NSC-34 cells is shown. Normalized firefly luciferase activity was represented relative to siCTRL-transfected cells (mean ± S.E.; $n = 8$; paired *t* test analysis; *, $p < 0.05$; **, $p < 0.01$).

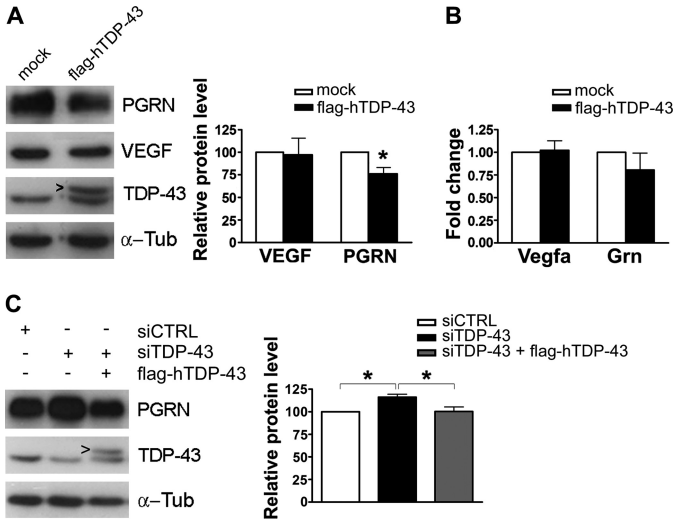

FIGURE 7. **Modulation of TDP-43 influences PGRN protein content.** *A*, shown is a representative Western blot of VEGF and PGRN in mock- and FLAG-hTDP-43-transfected NSC-34 cells (*left*) and densitometric analysis (mean ± S.E.; $n = 4$; paired *t* test analysis; *, $p < 0.05$) (*right*). The *arrowhead* indicates FLAG-hTDP-43 protein. *B*, real time PCR analysis of *Vegfa* and *Grn* mRNAs in mock- and FLAG-hTDP-43-transfected NSC-34 cells is shown. Fold change values for each gene were calculated *versus* mock-transfected samples (mean ± S.E.; $n = 4$). *C*, shown is a representative Western blot of rescue experiments with FLAG-hTDP-43 plasmid transfected for 24 h (*siTDP-43* + *FLAG-hTDP-43*) after a 48-h TDP-43 gene silencing (*siTDP-43*) (*left*) and densitometric analysis (*right*) (mean ± S.E.; $n = 4$; one-way analysis of variance and Tukey post hoc test; *, $p < 0.005$). α-Tubulin (*α-Tub*) was used for sample normalization.

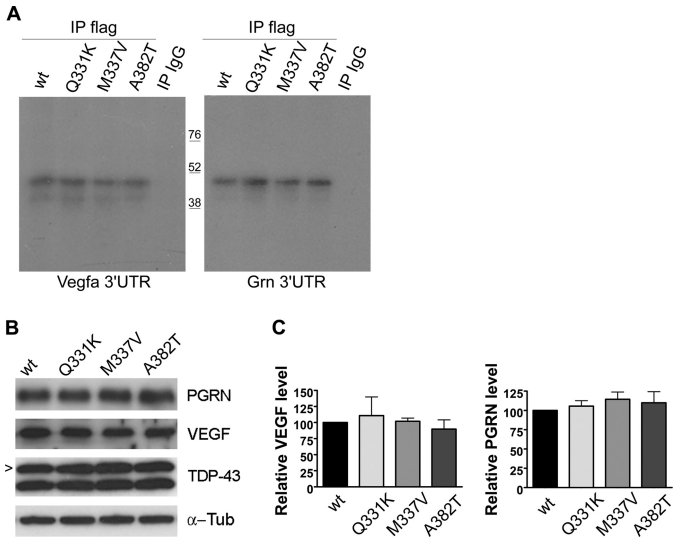

FIGURE 8. **Effect of TDP-43 mutants on the post-transcriptional regulation of *Vegfa* and *Grn* target mRNAs.** *A*, shown is a SDS-PAGE of UV-CLIP assay with wt or mutant (Q331K, M337V, A382T) FLAG-hTDP-43 and radiolabeled *Vegfa* (*left*) and *Grn* (*right*) 3′-UTR riboprobes. The isotypic IgG antibody was used as a negative control. *B*, shown is a representative Western blot of VEGF and PGRN in wt or mutant FLAG-hTDP-43-transfected NSC-34 cells (the *arrowhead* indicates FLAG-hTDP-43 protein). *α-Tub*, α-tubulin. *C*, shown is densitometric analysis of Western blot data (mean ± S.E.; $n = 5$; paired *t* test analysis).

As we found that TDP-43 is able to determine PGRN but not VEGF levels, rescue experiments were carried out to confirm such TDP-43-dependent post-transcriptional regulation of *Grn* mRNA. After TDP-43 knockdown, its gene expression was restored by transfection with the FLAG-hTDP-43 plasmid and PGRN protein content evaluated (Fig. 7*C*). We observed that the re-expression of TDP-43 restored PGRN content to a level comparable with that of mock-transfected cells (Fig. 7*C*).

As regards FUS, although our experimental data did not indicate any effect on its mRNA target stability, we investigated whether FUS depletion had any influence on the protein content of *Vps54*, whose mRNA we showed to be bound by FUS in its 3′-UTR sequence. We found that VPS54 protein levels did not change upon FUS gene-silencing in NSC-34 cells (supplemental Fig. 5).

Post-transcriptional Regulatory Effects of TDP-43 Mutants—To evaluate whether TDP-43 mutations may affect *Vegfa* and *Grn* mRNA binding, we tested the TDP-43 missense mutations Q331K, M337V, and A382T, previously reported in ALS patients (3, 50). Protein lysates from wild-type and mutant FLAG-hTDP-43-transfected NSC-34 cells were used in UV-CLIP experiments (Fig. 8*A*), and expression of the mutant recombinant proteins was assessed by Western blot assay (Fig. 8*B*). All the TDP-43 mutants analyzed showed no differences in the ability of binding *Vegfa* and *Grn* 3′-UTRs compared with the wild-type TDP-43 (Fig. 8*A*). By Western blot assays we also observed no differences in VEGF and PGRN protein levels in mutant TDP-43-transfected cells compared with the wild-type TDP-43 (Fig. 8*B*).

DISCUSSION

In this study, by utilizing a RIP-chip analysis, we defined and compared the mature mRNA targets or "targetome" of TDP-43 and FUS in the cytoplasmic compartment of motoneuron-like cells, which probably reflects a role of these two RBPs in RNA granule transport and local translation. Two distinct targetomes were identified for TDP-43 and FUS, and different post-transcriptional regulatory activities on their mRNA targets were demonstrated, suggesting that these two RBPs have distinct roles in neuronal RNA metabolism.

Importantly, recent findings have contributed to better understanding the role of TDP-43 and FUS in the pathogenesis of ALS and FTLD. Disease models in yeast and *Drosophila* indicate that these two proteins may have distinct and complementary roles in triggering cell toxicity and neurodegeneration (18, 51–54), although the issue of whether they have common or distinct functions in the brain is still open. Certainly, the full definition of their biological role and, therefore, of their RNA targets in neuronal cells may help understand why their dysfunction, probably associated to their mislocalization and aggregation in the cytoplasm, leads to selective neuronal death in ALS and FTLD.

The recent massive sequencing approaches utilized to identify the RNA targets of TDP-43 and FUS in brain tissues or in non-neural cells have confirmed and reinforced the role of these two RBPs mainly in pre-mRNA splicing activity. TDP-43 was found to recognize long intronic sequences endowed with $(UG)_n$ repeats (19–21), whereas FUS preferentially bound near splice site acceptors (23). However, the evidence that a smaller proportion of TDP-43 and FUS target sequences resides in the exonic and, more precisely, in the 3′-UTR sequences, also suggests that these two proteins may have additional roles in neuronal cells. In fact, similarly to the SMN protein, whose absence is causative of the infantile spinal muscular atrophy (SMA), TDP-43, and FUS RBPs, may have not only a nuclear activity associated to pre-mRNA splicing but also a role in mRNA transport and local translation in neurites, which may better account for neuronal cell death in ALS and FTLD diseases.

Several experimental findings already suggest that these two RBPs participate to transport of RNA granules in neurons and/or may control mRNA stability and translation. TDP-43 was described to bind and transport β-actin and calmodulin kinase II mRNAs to dendrites upon depolarization of hippocampal primary neurons and to regulate the stability of *Nfl* and its own transcript by binding to their 3′-UTR sequences (10, 25, 47). Similarly, FUS was shown to bind *Nd1-L* mRNA in its 3′-UTR and to move into dendrites upon NMDA stimulation (11, 12). The involvement of TDP-43 in controlling mRNA translation is based on the indirect evidence that it can be part of stress granules (15), the RNA triage site forming upon translational arrest induced by different cell stressors and containing stalled ribosomes, translation factors, and mRNAs as well as several RBPs (55). On the other hand, FUS forms stress granules only when it is mutated (16, 17, 56), and this supports the recent evidence that mutant FUS proteins, upon translocation into the cytoplasm, changes their targetome and preferentially binds 3′-UTR sequences (23).

TDP-43 has been described to co-localize with FUS mainly in nuclear complexes, and this interaction, which seems to be restricted to only 10% of cells, is greatly enhanced by mutant TDP-43 (57, 58). TDP-43 and FUS were reported to co-localize also in cytoplasmic RNPs (57), although the association of these proteins in the same RNP particle was rarely observed in our assays. Moreover, our RIP-chip data indicate that in the cytoplasm, TDP-43 and FUS recognize and bind distinct sets of mRNAs, suggesting that these two RBPs take part in distinct RNP complexes. Interestingly, we found that TDP-43 targets are enriched in transcripts associated to neuron-specific activities, whereas FUS targets are related to more general cellular activities, including DNA repair, cell cycle, and RNA processing, which have already been associated to FUS (59, 60). Although no common transcripts were identified from our analyses, the fact that some targets belonged to common GO categories indicates that TDP-43- and FUS-mediated post-transcriptional regulation may converge on the same cellular pathways.

In general, bioinformatics analyses of our data set revealed that the well known $(UG)_n$ consensus binding sequence for TDP-43 was present in the 3′-UTR of our RIP-chip-identified targets in about 80% of cases. However, other exonic regions may be responsible for TDP-43 binding, as already shown for *Hdac6* mRNA (61), and other consensus binding motifs may be present in such 3′-UTR sequences, as also supported by our computational analyses. The issue is more complicated for FUS because the MEME-identified binding motif was represented only in a very small subset of 3′-UTR target sequences, and the short GGUG consensus motif, previously identified by a SELEX analysis (32), was not consistently observed in our data set. It is also likely that FUS binding needs a particular folding and conformational structure of the target mRNA rather than a mere consensus sequence motif, as already suggested (12, 23). Nonetheless, by *in vitro* binding assays we have confirmed binding of FUS to the 3′-UTR of RIP-chip-identified targets in 3/5 selected cases, leaving again open the possibility of other exonic sequences being recognized and bound by FUS in these transcripts.

The RIP-chip analysis was suitable to our purpose to define the mRNA composition of TDP-43- and FUS-containing RNPs in the cytoplasmic compartment of NSC-34 cells. We confirmed some TDP-43 and FUS targets recently identified by other approaches and roughly mapped in exonic regions (19–21, 23), further suggesting that TDP-43 and FUS bind them as mature mRNAs. However, the targetomes we defined for TDP-43 and FUS may represent a subgroup of all their real targets. In fact, the discrepancy observed in the number of targets identified for TDP-43 and FUS might not reflect a difference in their RNA binding properties but more probably the different efficiency of the commercial antibodies used to recognize and immunoprecipitate these two proteins when they are complexed into RNP particles, as also observed in CLIP experiments (21, 22). This could also explain the reason why we did not identify some recently demonstrated TDP-43 and FUS targets as mature mRNAs (10, 25, 47, 61). Notwithstanding these caveats, the data emerging from our work undoubtedly contribute to better define the cytoplasmic targetome of TDP-43 and

FUS, a result that will certainly represent an important referential source to begin to unravel the pathogenic mechanisms involved in ALS and FTLD diseases. Nonetheless, as shown by our *in vitro* analyses, all these "-omics" data need to be carefully handled and to be experimentally validated in biological models.

In keeping with this consideration, in this work we have further investigated the role played by TDP-43 in regulating post-transcriptionally *Vegfa* and *Grn*, as they are genetically related to ALS and FTLD (33–35, 43, 44) and their reduced protein levels have been shown to trigger neuronal death (62, 63). We found that TDP-43, by binding to *Vegfa* and *Grn* 3′-UTR sequences, may control their mRNA stability and ultimately determine the content of PGRN protein. Also, the most common TDP-43 mutations reported in ALS patients (Q331K, M337V, A382T) had no effect on its binding activity of *Vegfa* and *Grn* target mRNAs.

Conversely, FUS binding to *Taf15*, *Nvl*, and *Vps54* 3′-UTRs seems to regulate neither the stability of its bound targets nor the content of VPS54 protein, for which an immunoblot was possible. Interestingly, this observation about FUS was already reported for the *Nd1-L* target, which was described to be transported into dendrites by FUS with no regulation of its mRNA stability (12).

Importantly, an increase in PGRN protein levels and no changes in VEGF content were also detected in post-mortem spinal cord tissues from ALS patients (48, 49), similarly to what we observed in our *in vitro* model of TDP-43 "loss of function" condition. Indeed, in "TDP-43 proteinopathy" the nuclear clearance of TDP-43 together with its sequestration into aggregates may determine reduced levels of its soluble and active form (64). Therefore, our experimental data provide a mechanistic explanation of what is observed in affected tissues of sporadic ALS and FTLD patients. Moreover, our results indicate that changes of TDP-43 levels may in turn change PGRN content, which needs to be strictly regulated to avoid neurodegeneration or cancer (65). We also postulate that the observed unchanged levels of endogenous VEGF upon TDP-43 depletion or overexpression may be determined by the delicate balance of different *trans*-acting factors, including miRNAs and the stabilizing ELAV RBPs (66), which exert a complex post-transcriptional regulation on the long *Vegfa* 3′-UTR.

In conclusion, the findings emerging from our work further support the idea that TDP-43 and FUS have different, but probably complementary, functions in the cytoplasmic compartment of neuronal cells, such as controlling mRNA transport, stability, and probably translation in the case of TDP-43 and mRNA transport into neuronal processes in the case of FUS. Post-transcriptional regulation of gene expression is a particularly complex and articulated mechanism, above all in highly specialized cells such as neurons, where an efficient and tight control of mRNA fate in the nucleus and in the cytoplasm together with its transport into neurites for local translation is important for their demanding metabolism. But most importantly, our study further highlights the potential importance of aberrant RNA metabolism as a direct cause of disease. In fact, considering the sheer number of potentially mysregulated targets/pathways after changes in cellular distribution of TDP-43 and FUS protein, it is very likely that even small alterations in the relative quantity of these proteins in the nucleus/cytoplasm might cause neurodegeneration over a long period of time (especially if we consider that the ability of cells to compensate for even small changes from normality gradually diminishes with age). One of the key research questions that studies such as ours will open up in the near future will be to correctly categorize and classify these aberrant events in terms of severity/importance with regard to the neurodegeneration process. This will in turn help to prioritize areas of therapeutic intervention.

Acknowledgment—We thank Dr. D. Gentilini for support in chip hybridization and data analysis.

REFERENCES

1. Neumann, M., Sampathu, D. M., Kwong, L. K., Truax, A. C., Micsenyi, M. C., Chou, T. T., Bruce, J., Schuck, T., Grossman, M., Clark, C. M., McCluskey, L. F., Miller, B. L., Masliah, E., Mackenzie, I. R., Feldman, H., Feiden, W., Kretzschmar, H. A., Trojanowski, J. Q., and Lee, V. M. (2006) Ubiquitinated TDP-43 in frontotemporal lobar degeneration and amyotrophic lateral sclerosis. *Science* **314,** 130–133
2. Arai, T., Hasegawa, M., Akiyama, H., Ikeda, K., Nonaka, T., Mori, H., Mann, D., Tsuchiya, K., Yoshida, M., Hashizume, Y., and Oda, T. (2006) TDP-43 is a component of ubiquitin-positive Tau-negative inclusions in frontotemporal lobar degeneration and amyotrophic lateral sclerosis. *Biochem. Biophys. Res. Commun.* **351,** 602–611
3. Sreedharan, J., Blair, I. P., Tripathi, V. B., Hu, X., Vance, C., Rogelj, B., Ackerley, S., Durnall, J. C., Williams, K. L., Buratti, E., Baralle, F., de Belleroche, J., Mitchell, J. D., Leigh, P. N., Al-Chalabi, A., Miller, C. C., Nicholson, G., and Shaw, C. E. (2008) TDP-43 mutations in familial and sporadic amyotrophic lateral sclerosis. *Science* **319,** 1668–1672
4. Mackenzie, I. R., Rademakers, R., and Neumann, M. (2010) TDP-43 and FUS in amyotrophic lateral sclerosis and frontotemporal dementia. *Lancet Neurol.* **9,** 995–1007
5. Lagier-Tourenne, C., Polymenidou, M., and Cleveland, D. W. (2010) TDP-43 and FUS/TLS. Emerging roles in RNA processing and neurodegeneration. *Hum. Mol. Genet.* **19,** R46–R64
6. van Blitterswijk, M., and Landers, J. E. (2010) RNA processing pathways in amyotrophic lateral sclerosis. *Neurogenetics* **11,** 275–290
7. Kawahara, Y., and Mieda-Sato, A. (2012) TDP-43 promotes microRNA biogenesis as a component of the Drosha and Dicer complexes. *Proc. Natl. Acad. Sci. U.S.A.* **109,** 3347–3352
8. Buratti, E., and Baralle, F. E. (2010) The multiple roles of TDP-43 in pre-mRNA processing and gene expression regulation. *RNA Biol.* **7,** 420–429
9. Colombrita, C., Onesto, E., Tiloca, C., Ticozzi, N., Silani, V., and Ratti, A. (2011) RNA-binding proteins and RNA metabolism. A new scenario in the pathogenesis of amyotrophic lateral sclerosis. *Arch. Ital. Biol.* **149,** 83–99
10. Wang, I. F., Wu, L. S., Chang, H. Y., and Shen, C. K. (2008) TDP-43, the signature protein of FTLD-U, is a neuronal activity-responsive factor. *J. Neurochem.* **105,** 797–806
11. Fujii, R., Okabe, S., Urushido, T., Inoue, K., Yoshimura, A., Tachibana, T., Nishikawa, T., Hicks, G. G., and Takumi, T. (2005) The RNA binding protein TLS is translocated to dendritic spines by mGluR5 activation and regulates spine morphology. *Curr. Biol.* **15,** 587–593
12. Fujii, R., and Takumi, T. (2005) TLS facilitates transport of mRNA encoding an actin-stabilizing protein to dendritic spines. *J. Cell Sci.* **118,** 5755–5765
13. Belly, A., Moreau-Gachelin, F., Sadoul, R., and Goldberg, Y. (2005) Delocalization of the multifunctional RNA splicing factor TLS/FUS in hippocampal neurones. Exclusion from the nucleus and accumulation in dendritic granules and spine heads. *Neurosci. Lett.* **379,** 152–157
14. Besse, F., and Ephrussi, A. (2008) Translational control of localized mRNAs. Restricting protein synthesis in space and time. *Nat. Rev. Mol.*

Cell Biol. **9,** 971–980
15. Colombrita, C., Zennaro, E., Fallini, C., Weber, M., Sommacal, A., Buratti, E., Silani, V., and Ratti, A. (2009) TDP-43 is recruited to stress granules in conditions of oxidative insult. *J. Neurochem.* **111,** 1051–1061
16. Bosco, D. A., Lemay, N., Ko, H. K., Zhou, H., Burke, C., Kwiatkowski, T. J., Jr., Sapp, P., McKenna-Yasek, D., Brown, R. H., Jr., and Hayward, L. J. (2010) Mutant FUS proteins that cause amyotrophic lateral sclerosis incorporate into stress granules. *Hum. Mol. Genet.* **19,** 4160–4175
17. Gal, J., Zhang, J., Kwinter, D. M., Zhai, J., Jia, H., Jia, J., and Zhu, H. (2011) *Neurobiol. Aging* **32,** 2323–2340
18. Da Cruz, S., and Cleveland, D. W. (2011) Understanding the role of TDP-43 and FUS/TLS in ALS and beyond. *Curr. Opin. Neurobiol.* **21,** 904–919
19. Sephton, C. F., Cenik, C., Kucukural, A., Dammer, E. B., Cenik, B., Han, Y., Dewey, C. M., Roth, F. P., Herz, J., Peng, J., Moore, M. J., and Yu, G. (2011) Identification of neuronal RNA targets of TDP-43-containing ribonucleoprotein complexes. *J. Biol. Chem.* **286,** 1204–1215
20. Tollervey, J. R., Curk, T., Rogelj, B., Briese, M., Cereda, M., Kayikci, M., König, J., Hortobágyi, T., Nishimura, A. L., Zupunski, V., Patani, R., Chandran, S., Rot, G., Zupan, B., Shaw, C. E., and Ule, J. (2011) Characterizing the RNA targets and position-dependent splicing regulation by TDP-43. *Nat. Neurosci.* **14,** 452–458
21. Polymenidou, M., Lagier-Tourenne, C., Hutt, K. R., Huelga, S. C., Moran, J., Liang, T. Y., Ling, S. C., Sun, E., Wancewicz, E., Mazur, C., Kordasiewicz, H., Sedaghat, Y., Donohue, J. P., Shiue, L., Bennett, C. F., Yeo, G. W., and Cleveland, D. W. (2011) Long pre-mRNA depletion and RNA missplicing contribute to neuronal vulnerability from loss of TDP-43. *Nat. Neurosci.* **14,** 459–468
22. Xiao, S., Sanelli, T., Dib, S., Sheps, D., Findlater, J., Bilbao, J., Keith, J., Zinman, L., Rogaeva, E., and Robertson, J. (2011) RNA targets of TDP-43 identified by UV-CLIP are deregulated in ALS. *Mol. Cell. Neurosci.* **47,** 167–180
23. Hoell, J. I., Larsson, E., Runge, S., Nusbaum, J. D., Duggimpudi, S., Farazi, T. A., Hafner, M., Borkhardt, A., Sander, C., and Tuschl, T. (2011) RNA targets of wild-type and mutant FET family proteins. *Nat. Struct. Mol. Biol.* **18,** 1428–1431
24. Keene, J. D. (2007) RNA regulons. Coordination of post-transcriptional events. *Nat. Rev. Genet.* **8,** 533–543
25. Ayala, Y. M., De Conti, L., Avendaño-Vázquez, S. E., Dhir, A., Romano, M., D'Ambrogio, A., Tollervey, J., Ule, J., Baralle, M., Buratti, E., and Baralle, F. E. (2011) TDP-43 regulates its mRNA levels through a negative feedback loop. *EMBO J.* **30,** 277–288
26. Ratti, A., Fallini, C., Colombrita, C., Pascale, A., Laforenza, U., Quattrone, A., and Silani, V. (2008) Post-transcriptional regulation of neuro-oncological ventral antigen 1 by the neuronal RNA-binding proteins ELAV. *J. Biol. Chem.* **283,** 7531–7541
27. Machanick, P., and Bailey, T. L. (2011) MEME-ChIP. Motif analysis of large DNA datasets. *Bioinformatics* **27,** 1696–1697
28. Bailey, T. L., Williams, N., Misleh, C., and Li, W. W. (2006) MEME. Discovering and analyzing DNA and protein sequence motifs. *Nucleic Acids Res.* **34,** W369–W373
29. Ayala, Y. M., Zago, P., D'Ambrogio, A., Xu, Y. F., Petrucelli, L., Buratti, E., and Baralle, F. E. (2008) Structural determinants of the cellular localization and shuttling of TDP-43. *J. Cell Sci.* **121,** 3778–3785
30. Buratti, E., and Baralle, F. E. (2001) Characterization and functional implications of the RNA binding properties of nuclear factor TDP-43, a novel splicing regulator of CFTR exon 9. *J. Biol. Chem.* **276,** 36337–36343
31. Ayala, Y. M., Pantano, S., D'Ambrogio, A., Buratti, E., Brindisi, A., Marchetti, C., Romano, M., and Baralle, F. E. (2005) Human, *Drosophila*, and *C. elegans* TDP43. Nucleic acid binding properties and splicing regulatory function. *J. Mol. Biol.* **348,** 575–588
32. Lerga, A., Hallier, M., Delva, L., Orvain, C., Gallais, I., Marie, J., and Moreau-Gachelin, F. (2001) Identification of an RNA binding specificity for the potential splicing factor TLS. *J. Biol. Chem.* **276,** 6807–6816
33. Lambrechts, D., Storkebaum, E., Morimoto, M., Del-Favero, J., Desmet, F., Marklund, S. L., Wyns, S., Thijs, V., Andersson, J., van Marion, I., Al-Chalabi, A., Bornes, S., Musson, R., Hansen, V., Beckman, L., Adolfsson, R., Pall, H. S., Prats, H., Vermeire, S., Rutgeerts, P., Katayama, S., Awata, T., Leigh, N., Lang-Lazdunski, L., Dewerchin, M., Shaw, C., Moons, L., Vlietinck, R., Morrison, K. E., Robberecht, W., Van Broeckhoven, C., Collen, D., Andersen, P. M., and Carmeliet, P. (2003) VEGF is a modifier of amyotrophic lateral sclerosis in mice and humans and protects motoneurons against ischemic death. *Nat. Genet.* **34,** 383–394
34. Baker, M., Mackenzie, I. R., Pickering-Brown, S. M., Gass, J., Rademakers, R., Lindholm, C., Snowden, J., Adamson, J., Sadovnick, A. D., Rollinson, S., Cannon, A., Dwosh, E., Neary, D., Melquist, S., Richardson, A., Dickson, D., Berger, Z., Eriksen, J., Robinson, T., Zehr, C., Dickey, C. A., Crook, R., McGowan, E., Mann, D., Boeve, B., Feldman, H., and Hutton, M. (2006) Mutations in progranulin cause Tau-negative frontotemporal dementia linked to chromosome 17. *Nature* **442,** 916–919
35. Cruts, M., Gijselinck, I., van der Zee, J., Engelborghs, S., Wils, H., Pirici, D., Rademakers, R., Vandenberghe, R., Dermaut, B., Martin, J. J., van Duijn, C., Peeters, K., Sciot, R., Santens, P., De Pooter, T., Mattheijssens, M., Van den Broeck, M., Cuijt, I., Vennekens, K., De Deyn, P. P., Kumar-Singh, S., and Van Broeckhoven, C. (2006) Null mutations in progranulin cause ubiquitin-positive frontotemporal dementia linked to chromosome 17q21. *Nature* **442,** 920–924
36. Elden, A. C., Kim, H. J., Hart, M. P., Chen-Plotkin, A. S., Johnson, B. S., Fang, X., Armakola, M., Geser, F., Greene, R., Lu, M. M., Padmanabhan, A., Clay-Falcone, D., McCluskey, L., Elman, L., Juhr, D., Gruber, P. J., Rüb, U., Auburger, G., Trojanowski, J. Q., Lee, V. M., Van Deerlin, V. M., Bonini, N. M., and Gitler, A. D. (2010) Ataxin-2 intermediate-length polyglutamine expansions are associated with increased risk for ALS. *Nature* **466,** 1069–1075
37. Maruyama, H., Morino, H., Ito, H., Izumi, Y., Kato, H., Watanabe, Y., Kinoshita, Y., Kamada, M., Nodera, H., Suzuki, H., Komure, O., Matsuura, S., Kobatake, K., Morimoto, N., Abe, K., Suzuki, N., Aoki, M., Kawata, A., Hirai, T., Kato, T., Ogasawara, K., Hirano, A., Takumi, T., Kusaka, H., Hagiwara, K., Kaji, R., and Kawakami, H. (2010) Mutations of optineurin in amyotrophic lateral sclerosis. *Nature* **465,** 223–226
38. Ticozzi, N., Vance, C., Leclerc, A. L., Keagle, P., Glass, J. D., McKenna-Yasek, D., Sapp, P. C., Silani, V., Bosco, D. A., Shaw, C. E., Brown, R. H., Jr., and Landers, J. E. (2011) Mutational analysis reveals the FUS homolog TAF15 as a candidate gene for familial amyotrophic lateral sclerosis. *Am. J. Med. Genet. B. Neuropsychiatr. Genet.* **156B,** 285–290
39. Schmitt-John, T., Drepper, C., Mussmann, A., Hahn, P., Kuhlmann, M., Thiel, C., Hafner, M., Lengeling, A., Heimann, P., Jones, J. M., Meisler, M. H., and Jockusch, H. (2005) Mutation of Vps54 causes motor neuron disease and defective spermiogenesis in the wobbler mouse. *Nat. Genet.* **37,** 1213–1215
40. Sharma, A., Lambrechts, A., Hao le, T., Le, T. T., Sewry, C. A., Ampe, C., Burghes, A. H., and Morris, G. E. (2005) A role for complexes of survival of motor neurons (SMN) protein with gemins and profilin in neurite-like cytoplasmic extensions of cultured nerve cells. *Exp. Cell Res.* **309,** 185–197
41. Gorba, T., Bradoo, P., Antonic, A., Marvin, K., Liu, D. X., Lobie, P. E., Reymann, K. G., Gluckman, P. D., and Sieg, F. (2006) Neural regeneration protein is a novel chemoattractive and neuronal survival-promoting factor. *Exp. Cell Res.* **312,** 3060–3074
42. Nagahama, M., Hara, Y., Seki, A., Yamazoe, T., Kawate, Y., Shinohara, T., Hatsuzawa, K., Tani, K., and Tagaya, M. (2004) NVL2 is a nucleolar AAA-ATPase that interacts with ribosomal protein L5 through its nucleolar localization sequence. *Mol. Biol. Cell* **15,** 5712–5723
43. Borroni, B., Ghezzi, S., Agosti, C., Archetti, S., Fenoglio, C., Galimberti, D., Scarpini, E., Di Luca, M., Bresolin, N., Comi, G. P., Padovani, A., Del Bo, R. (2008) Preliminary evidence that VEGF genetic variability confers susceptibility to frontotemporal lobar degeneration. *Rejuvenation Res.* **11,** 773–780
44. Sleegers, K., Brouwers, N., Maurer-Stroh, S., van Es, M. A., Van Damme, P., van Vught, P. W., van der Zee, J., Serneels, S., De Pooter, T., Van den Broeck, M., Cruts, M., Schymkowitz, J., De Jonghe, P., Rousseau, F., van den Berg, L. H., Robberecht, W., and Van Broeckhoven, C. (2008) Progranulin genetic variability contributes to amyotrophic lateral sclerosis. *Neurology* **71,** 253–259
45. Jiao, J., Herl, L. D., Farese, R. V., and Gao, F. B. (2010) MicroRNA-29b regulates the expression level of human progranulin, a secreted glycoprotein implicated in frontotemporal dementia. *PLoS One* **5,** e10551

46. Rademakers, R., Eriksen, J. L., Baker, M., Robinson, T., Ahmed, Z., Lincoln, S. J., Finch, N., Rutherford, N. J., Crook, R. J., Josephs, K. A., Boeve, B. F., Knopman, D. S., Petersen, R. C., Parisi, J. E., Caselli, R. J., Wszolek, Z. K., Uitti, R. J., Feldman, H., Hutton, M. L., Mackenzie, I. R., Graff-Radford, N. R., and Dickson, D. W. (2008) Common variation in the miR-659 binding-site of GRN is a major risk factor for TDP43-positive frontotemporal dementia. *Hum. Mol. Genet.* **17,** 3631–3642
47. Strong, M. J., Volkening, K., Hammond, R., Yang, W., Strong, W., Leystra-Lantz, C., and Shoesmith, C. (2007) TDP43 is a human low molecular weight neurofilament (hNFL) mRNA-binding protein. *Mol. Cell. Neurosci.* **35,** 320–327
48. Irwin, D., Lippa, C. F., and Rosso, A. (2009) Progranulin (PGRN) expression in ALS. An immunohistochemical study. *J. Neurol. Sci.* **276,** 9–13
49. Devos, D., Moreau, C., Lassalle, P., Perez, T., De Seze, J., Brunaud-Danel, V., Destée, A., Tonnel, A. B., and Just, N. (2004) Low levels of the vascular endothelial growth factor in CSF from early ALS patients. *Neurology* **62,** 2127–2129
50. Corrado, L., Ratti, A., Gellera, C., Buratti, E., Castellotti, B., Carlomagno, Y., Ticozzi, N., Mazzini, L., Testa, L., Taroni, F., Baralle, F. E., Silani, V., and D'Alfonso, S. (2009) High frequency of TARDBP gene mutations in Italian patients with amyotrophic lateral sclerosis. *Hum. Mutat* **30,** 688–694
51. Sun, Z., Diaz, Z., Fang, X., Hart, M. P., Chesi, A., Shorter, J., and Gitler, A. D. (2011) Molecular determinants and genetic modifiers of aggregation and toxicity for the ALS disease protein FUS/TLS. *PLoS Biol.* **9,** e1000614
52. Wang, J. W., Brent, J. R., Tomlinson, A., Shneider, N. A., and McCabe, B. D. (2011) The ALS-associated proteins FUS and TDP-43 function together to affect *Drosophila* locomotion and life span. *J. Clin. Invest.* **121,** 4118–4126
53. Lanson, N. A., Jr., Maltare, A., King, H., Smith, R., Kim, J. H., Taylor, J. P., Lloyd, T. E., and Pandey, U. B. (2011) A *Drosophila* model of FUS-related neurodegeneration reveals genetic interaction between FUS and TDP-43. *Hum. Mol. Genet.* **20,** 2510–2523
54. Kryndushkin, D., Wickner, R. B., and Shewmaker, F. (2011) FUS/TLS forms cytoplasmic aggregates, inhibits cell growth, and interacts with TDP-43 in a yeast model of amyotrophic lateral sclerosis. *Protein Cell* **2,** 223–236
55. Anderson, P., and Kedersha, N. (2008) Stress granules. The Tao of RNA triage. *Trends Biochem. Sci.* **33,** 141–150
56. Dormann, D., Rodde, R., Edbauer, D., Bentmann, E., Fischer, I., Hruscha, A., Than, M. E., Mackenzie, I. R., Capell, A., Schmid, B., Neumann, M., and Haass, C. (2010) ALS-associated fused in sarcoma (FUS) mutations disrupt Transportin-mediated nuclear import. *EMBO J.* **29,** 2841–2857
57. Kim, S. H., Shanware, N. P., Bowler, M. J., and Tibbetts, R. S. (2010) Amyotrophic lateral sclerosis-associated proteins TDP-43 and FUS/TLS function in a common biochemical complex to co-regulate HDAC6 mRNA. *J. Biol. Chem.* **285,** 34097–34105
58. Ling, S. C., Albuquerque, C. P., Han, J. S., Lagier-Tourenne, C., Tokunaga, S., Zhou, H., and Cleveland, D. W. (2010) ALS-associated mutations in TDP-43 increase its stability and promote TDP-43 complexes with FUS/TLS. *Proc. Natl. Acad. Sci. U.S.A.* **107,** 13318–13323
59. Wang, X., Arai, S., Song, X., Reichart, D., Du, K., Pascual, G., Tempst, P., Rosenfeld, M. G., Glass, C. K., and Kurokawa, R. (2008) Induced ncRNAs allosterically modify RNA-binding proteins in *cis* to inhibit transcription. *Nature* **454,** 126–130
60. Kovar, H. (2011) Dr. Jekyll and Mr. Hyde. The two faces of the FUS/EWS/TAF15 protein family. *Sarcoma* **2011,** 837474
61. Fiesel, F. C., Voigt, A., Weber, S. S., Van den Haute, C., Waldenmaier, A., Görner, K., Walter, M., Anderson, M. L., Kern, J. V., Rasse, T. M., Schmidt, T., Springer, W., Kirchner, R., Bonin, M., Neumann, M., Baekelandt, V., Alunni-Fabbroni, M., Schulz, J. B., and Kahle, P. J. (2010) Knockdown of transactive response DNA-binding protein (TDP-43) down-regulates histone deacetylase 6. *EMBO J.* **29,** 209–221
62. Van Damme, P., Van Hoecke, A., Lambrechts, D., Vanacker, P., Bogaert, E., van Swieten, J., Carmeliet, P., Van Den Bosch, L., and Robberecht, W. (2008) Progranulin functions as a neurotrophic factor to regulate neurite outgrowth and enhance neuronal survival. *J. Cell Biol.* **181,** 37–41
63. Sathasivam, S. (2008) VEGF and ALS. *Neurosci. Res.* **62,** 71–77
64. Dormann, D., and Haass, C. (2011) TDP-43 and FUS: a nuclear affair. *Trends Neurosci.*, in press
65. Gass, J., Prudencio, M., Stetler, C., and Petrucelli, L. (2012) Progranulin: An emerging target for FTLD therapies. *Brain Res.,* in press
66. Levy, N. S., Chung, S., Furneaux, H., and Levy, A. P. (1998) Hypoxic stabilization of vascular endothelial growth factor mRNA by the RNA-binding protein HuR. *J. Biol. Chem.* **273,** 6417–6423
67. Grillo, G., Turi, A., Licciulli, F., Mignone, F., Liuni, S., Banfi, S., Gennarino, V. A., Horner, D. S., Pavesi, G., Picardi, E., and Pesole, G. (2010) UTRdb and UTRsite (RELEASE 2010): a collection of sequences and regulatory motifs of the untranslated regions of eukaryotic mRNAs. *Nucleic Acids Res.* **38**(Database issue), D75–80